Proceedings of the Seventeenth International Conference on
Civil, Structural and Environmental Engineering Computing
Edited by: P. Iványi, J. Kruis and B.H.V. Topping
Civil-Comp Conferences, Volume 6, Paper 3.4
Civil-Comp Press, Edinburgh, United Kingdom, 2023
doi: 10.4203/ccc.6.3.4

Preliminary Numerical Simulation of Shaking Table Test on Shaft-Tunnel Junction in Liquefiable Soil

M. Sun and J. Zhang

Department of Civil Engineering, Xi'an Jiaotong University
Xi'an, China

Abstract

The main content of this paper is the preliminary numerical simulations of a 1*g* shaking table test on shaft-tunnel junction in liquefiable soil. In addition to the soil-structure models, a free-field model is also considered. They are all computed using the OpenSees platform, and the PM4Sand constitutive model is used to characterize the properties of liquefiable Fujian sand. The presented data include the excess pore pressure and the vertical displacements of the structures. It has been demonstrated that the difference between the uplifts of the shaft and the tunnel is quite significant, posing a potential threat to the seismic safety of this type of underground structures. These preliminary simulations make a reasonable prediction for the future shaking table test, thus contributing to the design, the execution, and the interpretation of the test.

Keywords: liquefaction, shaft-tunnel junction, OpenSees, soil-structure interaction, Fujian sand, PM4Sand.

1 Introduction

Many researchers have conducted in-depth studies on the interaction between the underground structure and the foundation soil when earthquake occurs in a liquefiable ground. Tokimatsu et al. [1] studied the floating failure mechanism of circular cross-section tunnels with different buried depths in liquefied sites combining FLAC numerical simulation with a centrifuge shaking table test. Tao et al. [2] conducted a series of shaking table tests on double-span subway tunnels in a

single-layer liquefiable soil. Chen et al. [3] carried out a shaking table test on the cross section of a three-arch subway station in liquefiable ground. Ozcebe et al. [4] conducted a centrifuge shaking table test on the seismic responses of a circular tunnel in a liquefied site, and the test results were numerically reproduced using the OpenSees platform. It can be seen that previous research on the seismic responses of underground structures in liquefiable soil mainly took the cross section of a tunnel or the standard section of an underground station as the subject.

However, in practical engineering, underground structure is not always composed of continuous linings or simple standard cross sections. For example, before the construction of shield-driven tunnels, it is necessary to build a shaft as the starting and ending points of the excavation by shield machine, thus forming a shaft-tunnel junction. Cross passage should be set up as an emergency escape channel between double-line parallel tunnels. There are also the connections of underground metro stations and the interval tunnels. These critical structures are very common in underground networks, and their dynamic soil-structure interactions (SSI) are very complex due to the unique features of the adjoining structures, especially in the context of liquefiable soil.

Shaking table test and numerical simulation are two of the main methods for studying the SSI of underground structures. The former can offer the opportunity to visually observe the behaviour and characteristic of the SSI [5,6]. The latter can be used for further analysis of the test results and provide a more detailed description of the SSI mechanisms. Therefore, the combination of these two methods will be adopted to achieve a better understanding of the SSI of shaft-tunnel junction in liquefiable ground. As a preliminary study before the actual shaking table tests, a series of numerical simulations are performed using OpenSees platform.

2 The Shaking Table Tests

1*g* shaking table tests are intended on a shaft-tunnel junction in liquefiable soil as well as the free field. The test is based on a prototype of typical utility tunnel. In the process of similarity design, the safety factor against uplift F_s is adopted as the criterion [7]

$$F_s = \frac{W+Q}{U_s+U_d+F} \tag{1}$$

where W is the weight of the underground structure; Q is the frictional resistance between the side walls of the structure and the surrounding subsoil; U_s is the buoyant force due to hydrostatic pressure; U_d is the uplift force due to excess pore water pressure caused by liquefaction; F is the seepage force transferred from the lower soil block underlying the structure. The principle is that the safety factor is consistent between the prototype and the model soil-structure systems, and a 1 / 20 geometric similarity ratio is found to be optimal.

Thus, the shaft model is tentatively designed with a width of 1.0 m, a height of 1.3 m, a longitudinal length of 1.0 m, and a wall thickness of 0.1 m. The circular tunnel model has the outer diameter and lining thickness of 0.6 m and 0.025 m,

respectively. The liquefiable ground will consist of saturated Fujian sand, which is widely used in liquefaction-related experiments [8-11]. A hexagonal shear box is used as the model container. The distance between two parallel sides of the hexagon is 2.4 m., and the box has a height of 5 m. The mass of the shear box is approximately 3.25 tons. The tests are scheduled to be conducted using the multi-point shaking table system in Tongji University. According to the size and the weight of the model structure and the shear box, it only needs to occupy one shaking table with the bearing capacity of 70 tons.

3 The Numerical Models

The numerical models are constructed using the OpenSees platform [12]. The non-linear dynamic behaviour of the liquefiable Fujian sand is simulated by the PM4Sand model. It is a highly sophisticated constitutive model specifically developed for the purpose of geotechnical earthquake engineering [13]. In OpenSees, 24 parameters are required to define a PM4Sand material. The target of the calibration process is 10 of them, and the rest 14 parameters are given the default values set by the developers.

The maximum and minimum void ratios of Fujian sand are measured to be $e_{\max}$ = 0.882 and $e_{\min}$ = 0.612, respectively. The mass density of the sand ρ is calculated by

$$\rho = \frac{e+G_s}{1+e} \tag{2}$$

where e is the initial void ratio; G_s is the specific gravity of the solids, and it is measured to be 2.65 for Fujian sand. The Poisson's ratio is given by

$$\nu = \frac{K_0}{1+K_0} \tag{3}$$

where K_0 is the lateral pressure coefficient obtained by

$$K_0 = 1 - \sin\pi\frac{\phi'_{cv}}{180} \tag{4}$$

where ϕ'_{cv} is the critical state friction angle, and it is measured to be 32.8° by undrained triaxial test.

Q and R are Bolton's constants. They define the critical state line in PM4Sand. Based on previous data of Fujian sand, they are determined to be 8.6 and 0.9, respectively [14]. G_0 is shear modulus constant. It controls the small-strain shear modulus of the sand and is estimated to be 800.

h_{p0} is the contraction rate parameter, and it is calibrated by comparing the *CRR* vs N_{liq} curves. Undrained cyclic triaxial (TRX) tests were conducted on samples of Fujian sand. The initial void ratio was 0.801, meaning a relative density of 30%. The samples underwent isotropic consolidation under a cell pressure of 50 kPa. The amplitude of the cyclic deviator stress q ranged between 14.0 kPa and 20.0 kPa, corresponding to cyclic stress ratios (*CSR*) from 0.074 to 0.148. Thus, a cyclic

resistance ratio (*CRR*) curve was established for Fujian sand by the *CSR* and the number of cycles to reach liquefaction N_{liq}. The contraction rate parameter h_{p0} is calibrated so that the numerically obtained CRR_{DSS} vs N_{liq} curve would match the one by the TRX lab tests. Because PM4Sand is only available in plane-strain formulation, undrained cyclic direct simple shear (DSS) tests are simulated under the initial effective vertical stress of 50 kPa. It must be pointed out that the *CRR* data are not directly comparable between the DSS and the TRX tests, so the following conversion is necessary [15]

$$CRR_{DSS} = \frac{2(1+2K_0)}{3\sqrt{3}} CRR_{TRX} \tag{5}$$

The comparison between the CRR_{DSS} converted from the TRX lab tests and the CRR_{DSS} simulated using PM4Sand is shown in Figure 1. The black curve is from the TRX tests after the above conversion, and the red one is obtained by the DSS simulations using PM4Sand. After numerous trials, it is found that h_{p0} = 0.250 could yield the best matched results. The calibrated constitutive parameters are summarized in Table 1.

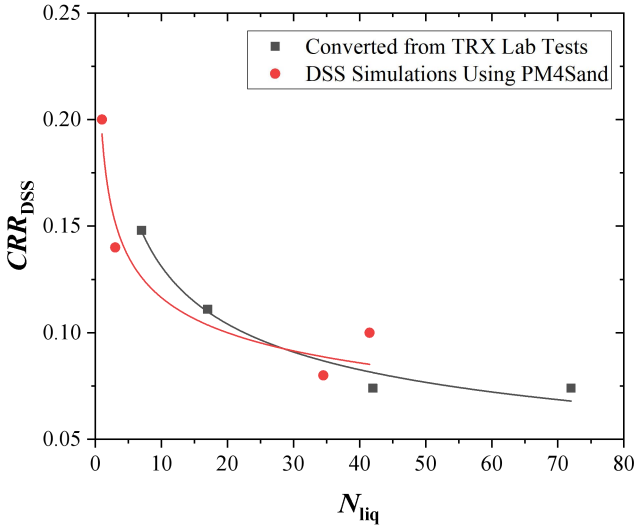

Figure 1: The converted and the simulated CRR_{DSS} vs. N_{liq} curves.

After the constitutive parameters have been properly calibrated, three plane-strain numerical models are constructed and computed as shown in Figure 2. The first one is a section of the free field, 2.4 m in width and 5.0 m in height, according to the dimensions of the shear box. The Fujian sand is modelled by quadrilateral displacement-pressure coupled elements termed as SSPquadUP elements [16]. The nominal element size of the mesh is 0.1 m. The main purpose of this model is for the nonlinear analysis of the liquefiable free field. The second model includes a cross section of the shaft in the same ground conditions. The width of the shaft is 1.0 m, and the height is 1.3 m. Its buried depth is 0.2 m below the surface. The third model is similarly constructed consisting of a circular cross section of the tunnel and the surrounding saturated Fujian sand. The diameter of the tunnel is 0.6 m, and the

depth of its crown is 0.7 m. In both SSI models, the structures are modelled by elastic beam elements, and the soil-structure contacts are defined as perfect ties.

Parameter	Description	Value for Fujian sand
D_r	Relative density	30%
G_0	Shear modulus constant	800
h_{p0}	Contraction rate parameter	0.250
ρ (Mg / m^3)	Mass density of Fujian Sand	1.94
e_{max}	Maximum void ratios	0.882
e_{min}	Minimum void ratios	0.612
ϕ'_{cv}	Critical state effective friction angle	32.8°
Q	Critical state line parameter	8.6
R	Critical state line parameter	0.9
ν	Poisson's ratio	0.31

Table 1: Calibrated constitutive parameters of PM4sand for Fujian sand.

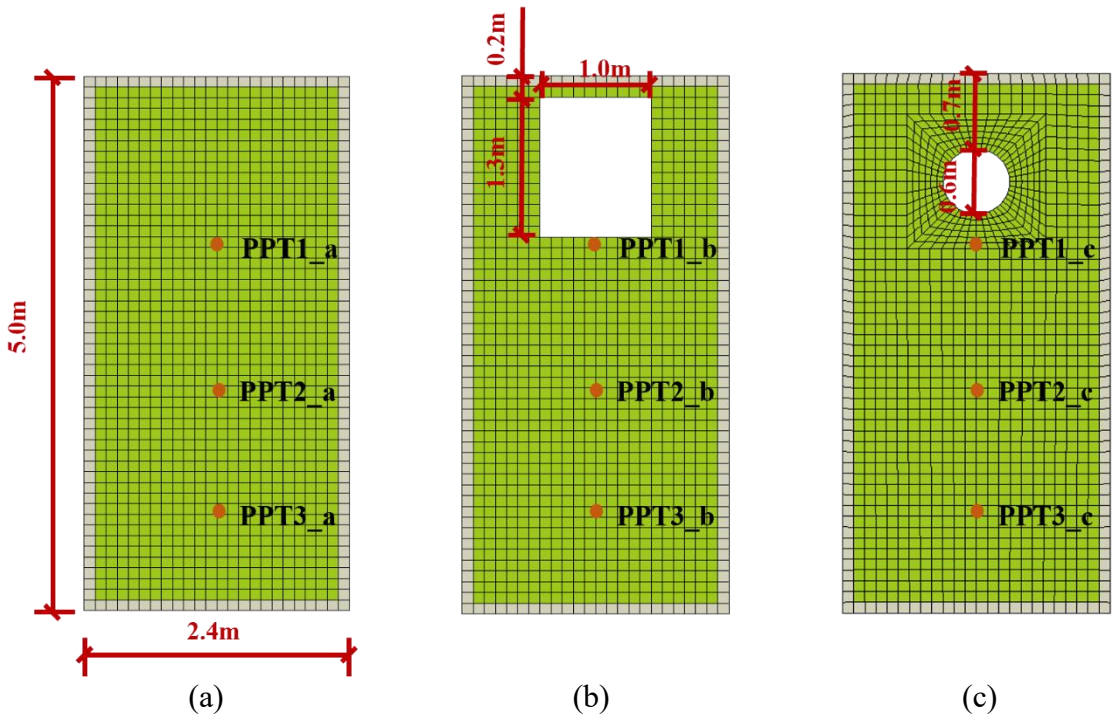

Figure 2: Plane-strain numerical models. (a) Free Field; (b) Shaft; (c) Tunnel.

In the above finite element models, the bottom edges are fixed in the vertical direction. A near-sinusoidal acceleration signal recorded in an actual centrifuge shaking test is adopted as the input excitation [17]. The waveform has an amplitude of 0.86*g* as shown in Figure 3. On the lateral boundaries, the translational degree-of-freedoms of the nodes at the same elevation are constrained to be the same,

simulating the working principle of the shear box. The free surface is defined with open drainage.

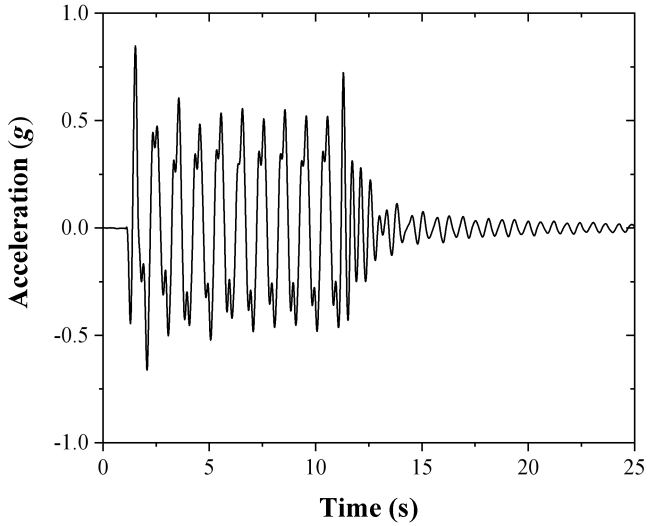

Figure 3: Input excitation for the numerical models.

4 Results

In the simulations, the vertical displacements of the structures and the pore pressure data of the sand are the main output. Through them, a reasonable prediction could be made for the future shaking table tests. In Figure 3, it can be observed that the vibration is more intense in the first 13 seconds, and the Fujian sand should be fully liquefied. Then, the vibration gradually ceases, and the liquefaction should diminish, too. The excess pore pressure (EPP) contours of the three models at 11 s are shown in Figure 4.

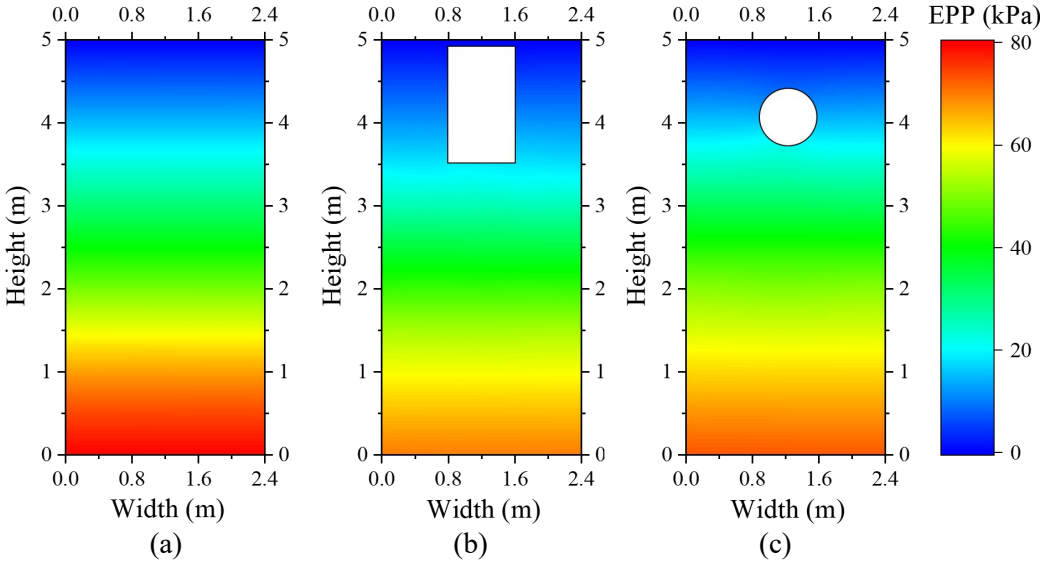

Figure 4: EPP contours at 11 s. (a) Free Field; (b) Shaft; (c) Tunnel.

It can be seen in Figure 4 that the EPP in the two SSI models are generally smaller than that of the free field. When the shaft or the tunnel is present, the flow of pore fluid and the behaviour of the surrounding sand will be affected by the dynamic SSI. It is possible that the structures could suppress the vibration, resulting in a decreased accumulation of EPP. It seems that the larger the cross-sectional area of the structure, the greater the impact on the EPP. In order to verify this statement, the time histories of the pore pressures at three positions, denoted by PPT in Figure 2, are shown in Figure 5.

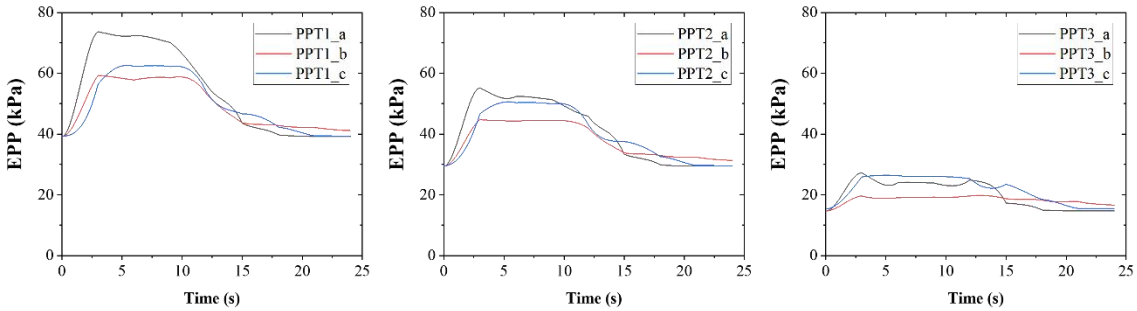

Figure 5: EPP build-up during the shaking.
(a) Pore pressure at PPT1; (b) Pore pressure at PPT2; (c) Pore pressure at PPT3.

In Figure 5, it can be clearly seen that the EPP accumulates to a lesser extent below both structures. Meanwhile, the larger cross section of the shaft has a greater effect. At PPT3, which is deepest, the influence of the smaller cross section of the tunnel is almost negligible.

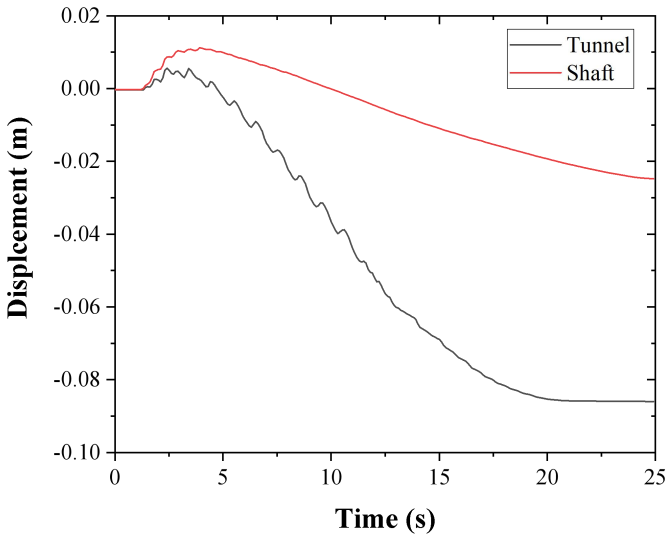

Figure 6: Time histories of the vertical displacements of the shaft and the tunnel by numerical simulations.

In addition to the EPP contours, the vertical displacements of the structures are extracted and plotted. It can be observed in Figure 6 that the vertical displacements of the shaft and the tunnel are quite different, and the uplift of the shaft is more prominent. According to Equation (1), the F_s of the shaft is much smaller than that of the tunnel because of the lesser EPP accumulation. With the vibration going on, the displacement gap between the two is growing. The discrepant responses between the two adjoining structures will be the focal point of the shaking table tests.

5 Conclusions

Three numerical models are computed using the OpenSees platform, offering a good prediction for the future shaking table tests.

Firstly, by analysing the EPP data, it is found that due to the presence of the structures, the EPP accumulation caused by the seismic shaking is reduced. The vertical displacements of the shaft and the tunnel are also shown. Although the shaft and the tunnel both uplifted in the liquefiable soil, the uplift displacements are quite different. The large displacement gap is very likely to cause structural damages on the adjoining structures. The numerical simulations will be of great importance for the design, the execution, and the interpretation of the future shaking table test.

Acknowledgements

The research was supported by the National Natural Science Foundation of China (52108383), the State Key Laboratory of Disaster Reduction in Civil Engineering (SLDRCE21-02), and the Fundamental Research Funds for the Central Universities (xzy012022075).

References

[1] S. C. Chian, K. Tokimatsu, S. P. G. Madabhushi, "Soil liquefaction–induced uplift of underground structures: physical and numerical modeling", Journal of Geotechnical and Geoenvironmental Engineering, 140(10), 04014057, 2014.

[2] C. Liu, L. Tao, J. Bian, Y. Zhang, J. Feng, "Shaking table test design for seismic response of liquefiable soil layer to soil-underground structure" , Journal of Disaster Prevention and Mitigation Engineering (06), 1341-1350, 2022.doi: 10.13409/j.cnki.jdpme.202004085

[3] G. Chen, S. Chen, C. Qi, X. Du, Z. Wang, W. Chen, "Shaking table tests on a three-arch type subway station structure in a liquefiable soil", Bulletin of Earthquake Engineering, 13, 1675-1701, 2015.

[4] A. G. Özcebe, D. Giretti, F. Bozzoni, V. Fioravante, C. G. Lai, "Centrifuge and numerical modelling of earthquake-induced soil liquefaction under free-field conditions and by considering soil–structure interaction", Bulletin of Earthquake Engineering, 19, 47-75, 2021.

[5] G. Chen, S. Chen, X. Zuo, C. Qi, X. Du, Z. Wang, "Shaking table model test on seismic response characteristics of subway station structure in soft soil site", Geotechnical mechanics (02), 331-342, 2016. doi:10.16285/j.rsm.2016.02.004

[6] W. Wu, M. Zhu, Y. Yuan, "Shaking table test on seismic dynamic earth pressure of multi-storey subway station", Urban rail transit research (08), 229-233, 2022. doi : 10.16037/j.1007-869x.2022.08.049
[7] J. Kosekt, O. Matsuo, Y. Koga, "Uplift behavior of underground structures caused by liquefaction of surrounding soil during earthquake", Soils and Foundations, 37(1), 97-108, 1997.
[8] T. Zhu, R. Wang, J. Zhang, "Effect of nearby ground structures on the seismic response of underground structures in saturated sand", Soil Dynamics and Earthquake Engineering, 146, 106756, 2021.
[9] C. Xu, Z. Zhang, Y. Li, X. Du, " Validation of a numerical model based on dynamic centrifuge tests and studies on the earthquake damage mechanism of underground frame structures", Tunnelling and Underground Space Technology, 104, 103538, 2020.
[10] H. Liu, W. Sun, Y. Zhang, W. Zhang, F. Han, W. Su, "Experimental analysis on the interaction between underground structures and sand layer under groundwater level change", Underground Space,2023.
[11] J. Fan, X. Zhao, J. Liu, B. Huang, " Seismic response of buried pipes in sloping medium dense sand", Soil Dynamics and Earthquake Engineering, 170, 107867, 2023.
[12] S. Mazzoni, F. McKenna, M. H. Scott, G. L. Fenves, "OpenSees command language manual", Pacific Earthquake Engineering Research (PEER) Center, 264(1), 137-158, 2006.
[13] R. W. Boulanger, K. Ziotopoulou, "PM4Sand (Version 3): A sand plasticity model for earthquake engineering applications", Center for Geotechnical Modeling Report No. UCD/CGM-15/01, Department of Civil and Environmental Engineering, University of California, Davis, Calif, 2015.
[14] J. Yang, H. Y. Sze, "Cyclic strength of sand under sustained shear stress", Journal of Geotechnical and Geoenvironmental Engineering, 137(12), 1275-1285, 2011.
[15] G. Castro, "Liquefaction and cyclic mobility of saturated sands", Journal of the Geotechnical Engineering Division,101, 551-569, 1975.
[16] C. R. McGann, P. Arduino, P. Mackenzie-Helnwein, "Stabilized single-point 4-node quadrilateral element for dynamic analysis of fluid saturated porous media", Acta Geotechnica, 7, 297-311, 2012.
[17] G. Miranda, V. Nappa, E. Bilotta, S. K. Haigh, G. S. Madabhushi, "Physical modelling of the interaction between a tunnel and a building in a liquefying ground and its mitigation", Tunnelling and Underground Space Technology, 137, 105108, 2023.